ELSEVIER

Journal of Archaeological Science 34 (2007) 358–373

Journal of Archaeological SCIENCE

http://www.elsevier.com/locate/jas

Sediments exposed to high temperatures: reconstructing pyrotechnological processes in Late Bronze and Iron Age Strata at Tel Dor (Israel)

Francesco Berna [a,*], Adi Behar [a], Ruth Shahack-Gross [a], John Berg [b], Elisabetta Boaretto [c], Ayelet Gilboa [d], Ilan Sharon [e], Sariel Shalev [a,f], Sana Shilstein [g], Naama Yahalom-Mack [e], Jeffrey R. Zorn [h], Steve Weiner [a]

[a] *Department of Structural Biology, Weizmann Institute of Science, Rehovot 76100, Israel*
[b] *Far Western Anthropological, Research Group, Inc., Davis, CA, USA*
[c] *Radiocarbon Dating and Cosmogenic Isotopes Laboratory, Weizmann Institute of Science, Rehovot 76100, Israel*
[d] *Zinman Institute of Archaeology, Haifa University, Haifa 31905, Israel*
[e] *Institute of Archaeology, Hebrew University of Jerusalem, Mt Scopus, Jerusalem, Israel 91905*
[f] *Institute of Marine Studies, Haifa University, Haifa 31905, Israel*
[g] *Department of Particle Physics, Weizmann Institute of Science, Rehovot 76100, Israel*
[h] *Department of Near Eastern Studies, Cornell University, Ithaca, NY, USA*

Received 31 March 2006; received in revised form 24 May 2006; accepted 24 May 2006

Abstract

Many of the sediments analysed from Tel Dor (Israel) show structural alterations indicating that they were exposed to high temperatures. This observation is consistent with the abundant evidence for use of pyrotechnology from the earliest exposed Middle Bronze Age strata through the Roman period. Such structurally altered sediments may well represent one of the more widespread and durable records of pyrotechnology, and as such could be invaluable for reconstructing past human activities. The specific aims of this research are therefore to develop the means for identifying local sediments that were altered by different pyrotechnological activities and to elucidate the varying circumstances whereby sediments were exposed to high temperatures in a Late Bronze and Iron Age 1 section.

We first characterize natural sediments sampled on and in the proximity of the *tell* and monitor their transformations due to exposure to high temperatures in an oven and in open fires, focusing in particular on the transformations of the clay mineral components of mud-brick materials. The analytical techniques used include micromorphology, Fourier transform infrared spectrometry (FTIR), X-ray powder diffractometry (XRD) and X-ray fluorescence (XRF) spectrometry. Using the temperature ''calibrated'' data, we confirm that large volumes of sediments at Tel Dor were exposed to high temperatures. In Area G, we identify three fundamentally different ways that heat-affected sediments were produced and accumulated: (1) In the Late Bronze Age (Phases 11–12) the sediments were heated to temperatures between 800 and 900 °C and were then deposited in the area under investigation. A plausible scenario is that these sediments were exposed to heat from ovens or kilns; (2) During the early Iron Age (Phase 10) the heat-affected sediments (heated above 1000 °C) formed in close association with casting pits for the working of copper-containing (bronze) objects. (3) During Phase 9 of the Iron Age, heat-affected sediments were produced *in situ* at this location due to a major conflagration. The temperatures reached around 1000 °C. This study shows that analysis of high temperature exposed sediments may be an invaluable means of reconstructing fire-associated activities, even when the actual installations have not been identified during the excavation or were not preserved.

Keywords: Burnt sediments; Heated clay minerals; Pyrotechnology; FTIR; XRF; Iron Age; Bronze Age; Tel Dor

* Corresponding author. Current address: Department of Archaeology, Boston University, 675 Commonwealth Avenue, Boston, MA 02215, USA. Fax: +1 617 353 6800.
E-mail address: fberna@bu.edu (F. Berna).

0305-4403/$ - see front matter © 2006 Elsevier Ltd. All rights reserved.
doi:10.1016/j.jas.2006.05.011

1. Introduction

An important aspect of human activity is the controlled use of fire. The benefits of using fire by humans are, of course, variable, and include cooked food, light and warmth in the earlier phases of fire use by hominids in the Paleolithic periods. In the later prehistoric and historical periods pyrotechnology was also used for the manufacture of materials and objects, such as the production of ceramics, plaster, metals and glass. Accidental or deliberately set fires, as well as pyrotechnology, leave their mark on the archaeological record. These include waste products like wood ash, charcoal, kiln wasters, slags, prills, etc. A rather neglected by-product of fire use is the sediment that was exposed to high temperatures. Such structurally altered sediments may well represent one of the more widespread and durable records of pyrotechnology, and as such could be invaluable for reconstructing past human activities.

This study was motivated by the observation that at Tel Dor, Israel (Fig. 1) many of the sediments analyzed by infrared spectroscopy showed indications of having been altered, presumably by exposure to high temperatures. This was initially inferred by comparing infrared spectra of sediments from various localities on the *tell* to the infrared spectra of Shoval [26,27] and Karkanas et al. [14] showing the effects of heat on clay structures using infrared spectroscopy. We therefore decided to investigate this subject in more detail both by performing a more systematic study on heat induced changes on the local *tell* sediments, and then by applying this methodology to the study of one exposed section. This section was chosen as it retained a record of several sequential stratigraphic phases that while excavating were observed to exemplify different uses of fire.

Sediments exposed to high temperature are structurally modified. This modification occurs to a very limited extent

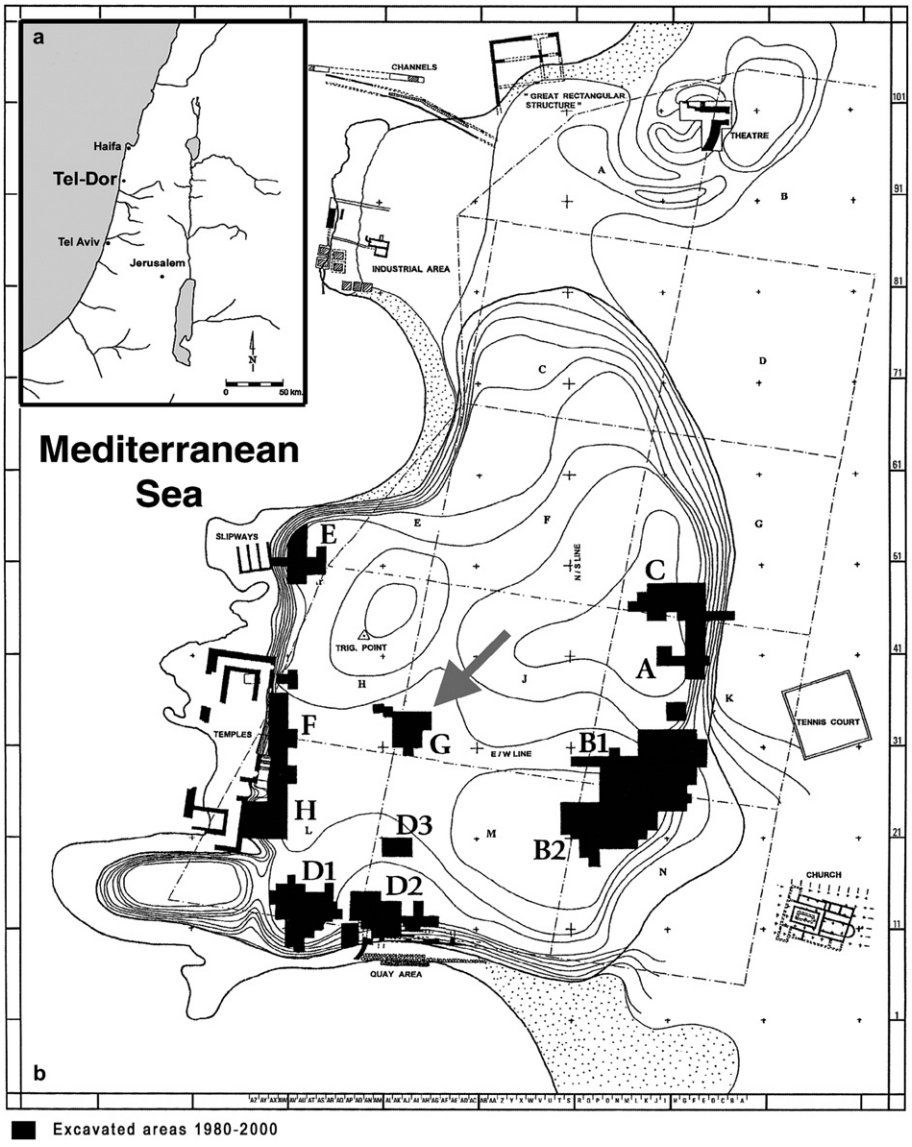

Fig. 1. Map showing the location of (a) the site of Tel Dor and (b) the location of Area G within the site.

if an open fire is made directly on the sediments [2], despite the fact that the temperature of such a fire can reach 900 °C [29]. The main reason is that as sediments are generally good insulators, the temperature even 1 cm beneath the fire rarely reaches 500 °C [2,6]. It occurs to a much greater extent if the temperature of the fire is elevated by the use of bellows. This is required for the smelting of metal from its ore mineral (i.e. the reduction of the metal to its metallic state), as this necessitates temperatures above the melting point of both rock (ca.1200 °C) and metal (copper 1083 °C, iron 1537 °C) [36]. Bellows are also required for copper (bronze) re-melting, temperatures in the range of 1000–1200 °C are necessary, depending on the alloying type [15]. The early production of glass was based on silica as the network former, soda as the alkali flux, and lime and magnesium as stabilizers. Tite et al. [32] have suggested for such mixtures a furnace temperature in the range of 1100–1200 °C, which is well beyond the required range for pottery production. Thus temperature alone is unlikely to definitively differentiate between various pyrotechnological practices. Clearly, the associated materials and archaeological context also need to be taken into account. Temperature however is an important parameter to help identify ancient pyrotechnologies.

Identifying the temperature range at which a sediment was burned is largely based on characterizing the irreversible transformations that occur due to the firing of silicate minerals, and in particular clay minerals. Clays undergo several structural and compositional changes when exposed to increasing temperatures [19]. Up to 200 °C adsorbed water evaporates. When the temperature increases to 450–600 °C, dehydroxylation and the loss of structurally bound water occur. In kaolinite this takes place rather abruptly, whereas for other clay types such as smectite and illite, structural water loss is more gradual. At this stage clay minerals become hard, although their porosity is still high. At 950 °C crystallization of new phases such as aluminosilicate spinel [$Si_8Al_{16}O_{32}$] occurs while porosity rapidly diminishes and the initiation of the glassy phase (amorphous free silica [SiO_2]) of the ceramic starts [7,20]. At higher temperatures (1000–1400 °C) mullite [$3Al_2O_3 \cdot 2SiO_2$] and polymorphs of SiO_2 such as tridymite and cristobalite form [7]. Quartz can also be transformed into its high temperature polymorphs even below the melting point of its pure state, due to the presence of alkali. One such example was reported by Shoval [27] in ceramic kiln walls.

Clay minerals are the main components in the industrial manufacturing of ceramics and bricks. Hence the above transformations have been widely studied by techniques such as differential thermal analysis (DTA)/thermogravimetric analysis (TGA), X-ray diffraction (XRD), nuclear magnetic resonance (NMR), Raman spectroscopy and Fourier transform infrared spectroscopy (FTIR) [1,3,9,18,28,34], for a range of temperatures up to 1400 °C. Here, we use this body of knowledge to study the effects of heat on clay-rich sediments from the archaeological site of Tel Dor in order to reconstruct the different human activities that were responsible for the heat exposure. We focus on the use of infrared spectroscopy for this purpose, as FTIR can be conveniently used on-site in an interactive manner as the excavation proceeds.

1.1. The site of Tel Dor

Tel Dor is a large mound located on the Mediterranean coast about 30 km south of Haifa (Fig. 1). It is identified with *D-jr* in Egyptian sources of the second millennium BCE, Biblical Dor, and with Dora in Greek and Roman sources. The occupational history of the site begins in the Middle Bronze Age and ends in the Crusader period [31]. Dor has one of the few good natural ports along Israel's coast and was a cross-road between the Mediterranean cultures to the west and those of the ancient Near East through all represented periods.

Near Eastern *tells* are occupational sites characterized by recurrent cycles of construction of durable (stone and/or brick) architecture, prolonged use of that architecture and varied events of constructional alterations, destructions and/or abandonment before another cycle of construction. Almost all the sediments on a *tell* are human-made or human-modified. This mainly includes building materials (stone, wood and mud-bricks); constructional fills for intentional leveling and filling (either re-deposited *tell* sediments or materials brought in from outside) and gradually accumulating anthropogenic waste. Since sun-dried mud-bricks can contain up to 45% clay, the result is a significant enrichment of the *tell* sediments in clays as compared to the adjacent environment [21]. Large- and small-scale construction involved substantial shifting of debris. The result is that many sediments on *tells* are in secondary (or further) deposition.

Dor is built partly on a *kurkar* (calcified sand dunes of Pleistocene age) ridge and partly on a *tombolo* – a sand spit that accumulated between this ridge and the coastline, forming a landscape of alternating capes and sheltered bays. Natural clay exposures in this environment are few (nowadays mostly in stream terraces some distance from the site), although there are Pleistocene clay deposits under the sand cover in the bays [13]. These may have been exposed in former times and mined for mud-brick material. Construction on the *tell* in the Bronze and Iron Ages is largely of mud-bricks, often on stone socles (either local *kurkar* or limestone brought in from the Carmel about 5 km away, or from stream beds). There is increasing use of stone, particularly ashlars (hewn *kurkar* blocks in pre-cut sizes), throughout the Iron Age and it becomes the dominant mode of construction in the ensuing Persian and Hellenistic periods. In the Roman period concrete is a significant construction material. These shifts in the dominant construction materials are directly reflected in the matrix of *tell* sediment. Quartz (from sand and degraded *kurkar*) is common throughout, but clay, most probably derived from degraded mud-brick and mud-plaster, forms a significant proportion of the sediments, but decreases in strata later than the Iron Age. As mud-bricks and mud-plaster are not produced by high temperatures, they can clearly be differentiated from sediments that have been exposed to fire.

Evidence for the use of pyrotechnology is abundant on the *tell*. In addition to many *tabuns* (cooking ovens) there is evidence for pottery production, lime was produced for use as plaster and cement, and glass and faience were also possibly produced locally. The purple dye industry based on *Murex* shells, for which there is also much evidence, requires heating as a part of the process. Evidence for metallurgical industries has been found at Tel Dor in the form of prills, slags, crucibles and *tuyer* fragments. There are also many fire-related installations whose functions are not presently known. We therefore decided to better understand the relations between the burned sediments and the pyrotechnological activities that could be responsible for their formation. We focused on a particular area at Tel Dor, namely the eastern section of Area G in the center of the *tell* (Figs. 1 and 2).

The specific aims of this research are: (1) to develop the means for identifying the local sediments that were altered by different pyrotechnological activities; (2) to distinguish between *in situ* burnt sediments and those that were re-deposited; as burnt sediments are ubiquitous on the *tell*, this is a major concern. (3) To improve our understanding of the specific activities involving fire recorded in Area G.

2. Materials and methods

Natural sediments were sampled in the proximity of Tel Dor. These include samples from the beach sand, rock outcrops, soils and sediments. We regard these as control samples that represent the natural environment without anthropogenic influences. Hundreds of "point" samples were obtained from freshly exposed surfaces of various archaeological features and strata on the *tell* in several excavation areas (e.g., Areas D1, D2, G). Archaeological mud-brick materials were sampled in bulk in Area G and Area D2. Clay mineral standards used in this study are: montmorillonite (Otay, California), kaolinite (Yang Shan, Suzhon, China) and illite (48W1535, Fithian, Illinois).

2.1. Particle size analysis and clay size fraction separation

Since clays are the most temperature sensitive component in the sediments, we analyzed them separately. The clay fraction of the mud-brick material was separated by the pipette method [10]. Samples were first sieved sequentially and the fraction smaller than 63 μm was then separated according to Stoke's law by suspension in a water column. The clay minerals were identified by combining FTIR and XRD analysis. The relative proportion of the different components was estimated by anlysing known mixtures of standard minerals.

2.2. Fourier transform infrared spectrometry (FTIR)

FTIR spectrometry was conducted both on-site, as well as in the laboratory, using a portable spectrometer (MIDAC M400). Representative FTIR spectra were obtained by grinding a few tens of micrograms of sample using an agate mortar and pestle. About 0.1 mg or less of the sample was mixed with about 80 mg of KBr (IR-grade). A 7 mm pellet was made using a hand press (Qwik Handi-Press, Spectra-Tech Industries Corporation) without evacuation. The spectra were collected between 4000 and 400 cm^{-1} at 4 cm^{-1} resolution.

2.3. X-Ray powder diffractometry (XRD)

XRD was mainly used for the determination of the clay mineralogy. Analysis was carried out using a Rigaku RU-200B Rotaflex instrument, with Cu-kα radiation. Powdered samples were measured in the range of two-theta (2-60 degrees), at a rate of 0.5 degree per min, and a sampling interval of 0.05.

2.4. X-ray fluorescence (XRF) spectrometry

The metal contents of bulk samples and charcoal fragments were analyzed by XRF. A portable bench spectrometer equipped with a Rhodium X-ray tube (EX-310LC, Jordan Valley,

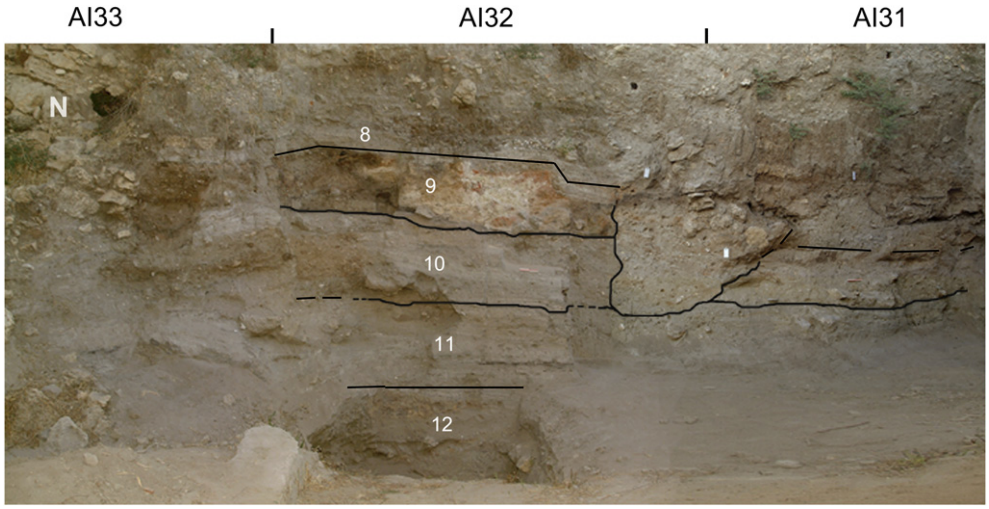

Fig. 2. Photograph of part of the eastern section of Area G with excavation square numbers and archaeological phase boundaries.

Israel) was used. For semi-quantitative determinations of total copper concentration in bulk sediments and in charcoal, calibration curves were prepared using standards prepared by mixing soil and graphite with a known weight percent concentration (wt%) of CuO. The detection limits for the content of CuO are about 0.01 wt% in sediment and 0.003 wt% in charcoal. The accuracy of the calibration was confirmed by ICP-OES elemental analysis after total dissolution of the samples in microwave digestors.

2.5. Micromorphology

Undisturbed sediment blocks were carved out of the eastern section of Area G (as well as from other locations in Area G) for micromorphological analysis. Due to the great height of the section, the samples do not represent a full, uninterrupted sequence. The carved blocks were coated with Plaster of Paris prior to their detachment from the profile in order to keep them intact during transportation to the laboratory, where they were impregnated with a polystyrene mixture. After polymerization they were cut using a rock saw and sent for thin section preparation to Spectrum Petrographics Inc. (Oregon, U.S.A.). Thin sections (standard 30 μm thickness) were examined using a polarizing light microscope (Nikon Labophot2-pol) and described, following Bullock et al. [4] and Courty et al. [8].

2.6. Oven experiments

Archaeological mud-brick material, the clay size fraction separated from the mud-brick material, and the standard clay mineral were heated. Each sample was heated in a porcelain crucible for 4 h in a muffle furnace at temperatures between 300 and 1300 °C in an air atmosphere. The samples were cooled and equilibrated at ambient temperature for several hours before being analyzed.

2.7. Open fire experiments in the field

The effect of the heat on the sediments due to different pyrotechnological activities was investigated at Tel Dor by performing experiments under conditions that simulate three possible conditions: (1) simple ‘‘domestic’’ fire, (2) fire augmented with one bellow, (3) fire augmented with two bellows for melting bronze scrap objects in a crucible.

These experiments were conducted using mechanical bellows propelled by an electrical fan. The constant airflow rate was about 20 L air per second. Each firing experiment was performed on an experimental bed prepared with archaeological mud-brick material. Pits of $1 \times 1 \times 0.5$ m were cleared and filled with compacted mud-brick material sampled from an Iron Age accumulation unearthed in excavation Area D2 (sample FX3-1). A charge of 2.0 kg of charcoal from local wood was piled and lighted. The temperature of the fire and of the sediment was monitored with thermocouple sensors connected to a digital thermometer. One thermocouple sensor was used to monitor the maximum temperature of the fire, while the second thermocouple was used to measure the temperature in the sediment under and around the fire. The experiments ended once the charcoal charge was completely exhausted. The sediments were left to cool and equilibrate with ambient conditions for 16 h before being sampled and analyzed.

3. Results

3.1. Heat-altered sediments at Tel Dor are widespread

Fig. 3 shows a selection of infrared spectra from different strata in Areas D and G that show features consistent with having been exposed to high temperatures. Farmer [9] and Shoval

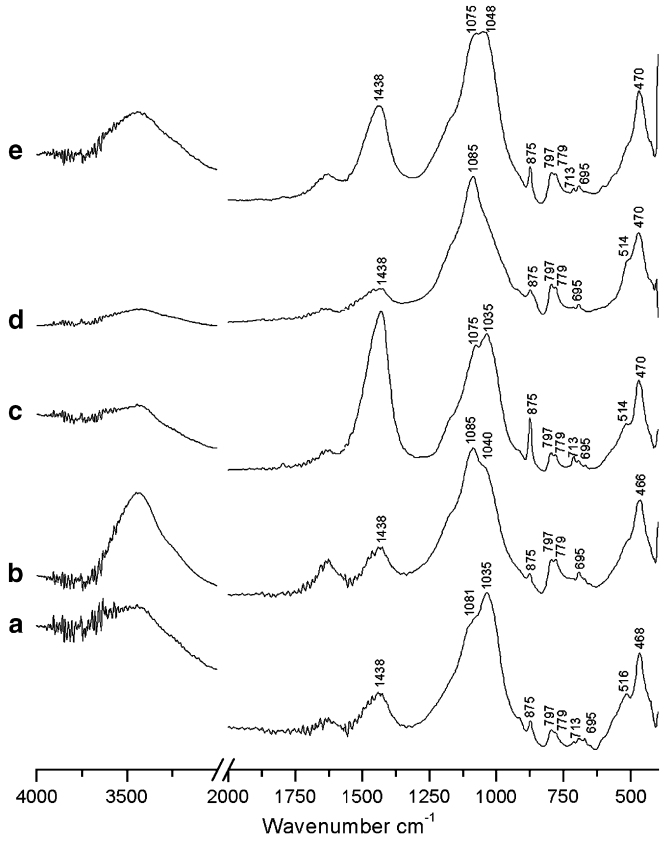

Fig. 3. Infrared spectra of sediments from different locations at Tel Dor that show features consistent with having been exposed to high temperatures. (a) Unburned sediment from the top of Phase 11 Area G east section (Figs. 2 and 8) showing unaltered clay and quartz peaks. Note the major clay absorption at 1035 cm^{-1} and the small kaolinite absorption peaks around 3600 cm^{-1}. (b) Sediment from the bottom of Phase 12c Area G east section (Figs. 2 and 8) from the Late Bronze Age. The spectrum shows the shift of the main Si–O–Si absorption of clay to higher wavenumbers and the disappearance of the 520–530 cm^{-1} and koalinite peaks. (c) Sediment from an industrial heat installation in Area D1 (Roman Period) showing calcite peaks (1430, 875 and 713 cm^{-1}), as well as clay peaks. The presence of the shoulder at 1075 cm^{-1} and the weak 514-cm^{-1} peak are indications of heat alteration. (d) White-colored sediment from the Phase 9 destruction layer in the east section of Area G (Figs. 2 and 8). The broad major absorption at 1085 cm^{-1}, the strong doublet at 797 and 779 cm^{-1} and the weak 514-cm^{-1} peaks are indications of heat alteration. (e) Sediment from a seventh century pit in Area D2. This spectrum shows the formation of a glassy phase identified by the broad band at 1050–1075 cm^{-1}, the complete lack of an absorption peak around 514 cm^{-1} and a poorly differentiated doublet at 797 and 779 cm^{-1}.

[26,27] have reported differences in infrared spectra of sediments that can be attributed to the effect of heating. These can be compared to spectrum 3a that is from sediment that was not exposed to high temperatures. The most conspicuous differences between the altered and unaltered sediments are:

(1) The shift of the major absorption peak from that of clay (around 1033 cm^{-1}) to higher wave numbers.
(2) The loss of the clay minerals peaks in the region of 3600 cm^{-1}.
(3) A weak absorption peak around 510 cm^{-1}.
(4) The 796 and 779 cm^{-1} doublet is relatively strong.

We initially identified heat-altered sediments in a section within an Iron Age monumental building in Area D2 [22]. Since then we have recognized such sediments in other locations within D2, in Area G, and in sediments from the Roman period in D1. Although a systematic study of their distribution has not been undertaken, it is clear that they are present in large amounts on the *tell*.

As the observed differences between burned and unburned sediments vary according to the proportions of quartz and clay minerals in the sediments, and according to the specific assemblage of clay minerals, we "calibrated" the effect of heating by subjecting local sediments to high temperatures in an oven and in open fires. We then use this information to assess the extent of heat exposure of sediments in the eastern section of the Area G.

3.2. Heating experiments

3.2.1. Materials characterization prior to heating

As the local landscape around Tel Dor has changed radically in the last few thousand years [13], it is difficult to identify sediments that would have been accessible to the inhabitants of the Tel during the Late Bronze and Iron Age periods. We therefore used mud-brick material brought to the *tell* during those periods, on the assumption that they represent the accessible sediments of the area. Table 1 shows the particle size distributions of six mud-brick materials from different locations on the tell. Micromorphological analysis shows that mud-bricks sampled in Area G are composed of clay, silt and sand-sized quartz grains. In Area G, some also contain *kurkar* fragments and even a few bone fragments. None of them show any indication from infrared spectra of having been exposed to high temperatures. The composition of mud-bricks from Area D2 is different from those in Area G and strongly resembles the Mediterranean soil type *Hamra* that develops on the local *kurkar* ridges. It is characterized by a grano-striated birefringence fabric [33]. The *kurkar* and bone containing mud-bricks in Area G were either produced differently (i.e., raw material has been manipulated) or their material acquired from a different, yet unidentified, source. The mud-brick materials represented by samples FX3-1 and WD2A15 are widespread in the archaeological layers of Tel Dor, especially in the Iron Age strata. We therefore chose FX3-1 for our detailed heating experiments. Its infrared spectrum is shown in Fig. 4a. It has the characteristic absorptions of kaolinite (3695, 3650, 3620 cm^{-1}), montmorillonite (3630, 1035, 915, 530 cm^{-1}), of small amounts of quartz (shoulder at around 1085, peaks at 797, 779, 695 and 510 cm^{-1}) and of calcite (1425, 875, 713 cm^{-1}).

3.2.2. Heating mud-brick sediment in an oven

The infrared spectra of archeological mud-brick material (sample FX3-1) heated for 4 h to different temperatures are shown in Fig. 4 (see figure legend for detailed changes in the spectra). The effect of exposure to high temperatures on the mud-brick material is readily discernible and the changes are consistent with those observed in the archaeological sediments (Fig. 3), as well as spectra of heated clays [9] and of heated kaolinite and smectite containing local soil [26,27]. This confirms the notion that large quantities of sediments at Tel Dor were affected by pyrotechnological activities. With a more detailed understanding of the transformation processes, it might also be possible to estimate the temperatures to which the sediments were exposed. As the clay minerals are clearly most susceptible to changes during heating, we studied clay fractions separated from mud-brick material.

3.2.3. Heating only the clay fraction of mud-brick sediments in an oven

The major mineralogical components of the clay size fraction of archaeological mud-brick material (sample FX3-1) are montmorillonite (>85%), kaolinite and a small amount of clay-sized quartz (Table 1). We separated the clay-sized fraction and then heated it for 4 h to different temperatures and

Table 1
Provenience and characterization of some archaeological mud-brick materials collected at Tel Dor

Sample		Location		Particle size (weight %)			Clay size fraction mineralogy[a]
Name	Description	Area	Phase	Sand	Silt	Clay	
FX3-1	Dark brown	D2	D2/8	56	16	28	S, K, Q
AI33-12	Yellowish	G	G/9	50	34	15	S, K, Q
AI33-13	Reddened	G	G/9	69	22	9	K, S, Q
AI33-14	Grey sandy	G	G/9	86	8	6	K, I, ?
AI33-15	Rammed earth	G	G/10	65	–	9	K, Q
WD2A15	Dark brown	D2	D2/8	47	26	27	S, K, Q

[a] S, smectite–montmorillonite; K, kaolinite; I, illite; Q, quartz.

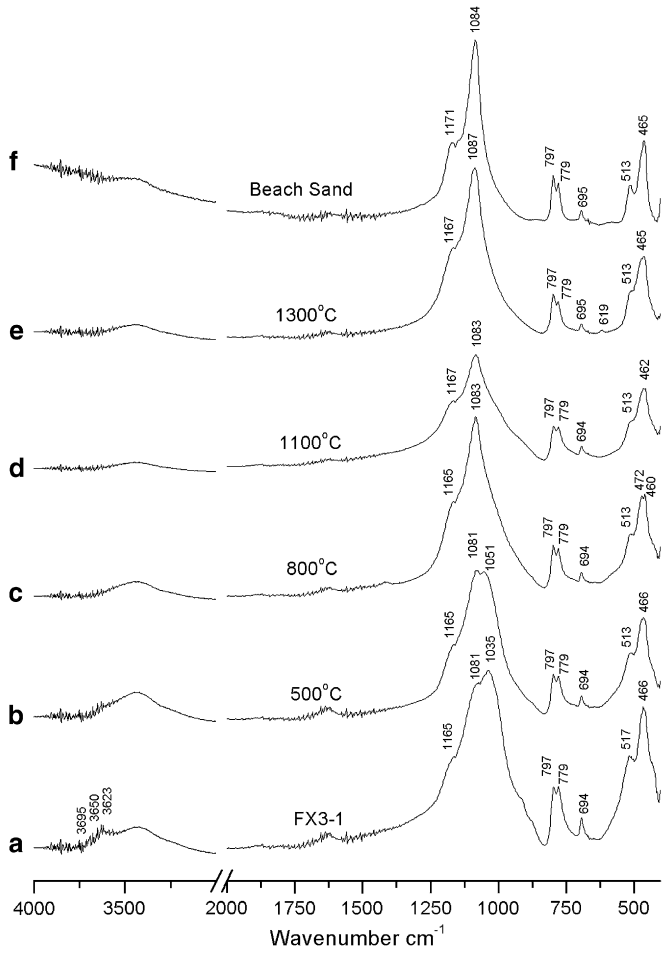

Fig. 4. Infrared spectra of the representative mud-brick material (Sample FX3-1) heated in an oven for 4 h to different temperatures. (a) Not heated; (b) Heated at 500 °C: the kaolinite absorption bands at 3695, 3650, 3620 cm^{-1} disappear due to the collapse of the structure due to the loss of hydroxyl groups. The strong Si–O–Si absorption peak at 1032 cm^{-1}, typical of clay minerals, shifts to 1050 cm^{-1}; the OH deformation band (Al–Al–OH) at 915 cm^{-1} disappears. The smectite–kaolinite Si–O–Al band at 520–530 cm^{-1} is substituted by the quartz Si–O band at 512 cm^{-1}. As a consequence, the valley between the resulting 512 cm^{-1} peak and the clay Si–O band at 470 cm^{-1} is not as well defined as for the unburned material. At the same time the Si–O–Si absorption of quartz (1082 cm^{-1}) as well as the doublet at 798 and 780 cm^{-1} (Si–O stretching) and 460 cm^{-1} peak (Si–O bending) become stronger and clearly distinguishable; (c) heated to 800 °C: the absorptions at 1040–1050 cm^{-1} disappear and the spectrum resembles that of quartz (1170, 1083, 797–780 doublet, 694, 460 cm^{-1}). A careful comparison with the quartz spectrum of quartz sand collected on the beach near Tel Dor (Fig. 4f) does however reveal subtle differences. The valley between the 460 and 512 cm^{-1} peaks is not as well defined as in beach sand quartz; (d) Heated at 1100 °C: The 512 cm^{-1} absorption is very week, the peaks of the 797–780 cm^{-1} doublet are elevated and equal in height, the major absorption peak at 1085 cm^{-1} is broad and has a distinct tailing towards lower wavenumbers; (e) Heated to 1300 °C: The main Si–O–Si absorption is shifted to 1087 cm^{-1} and a band at 617 cm^{-1}, characteristic of cristobalite, appears. (f) Spectrum of beach sand collected in the proximity of Tel Dor.

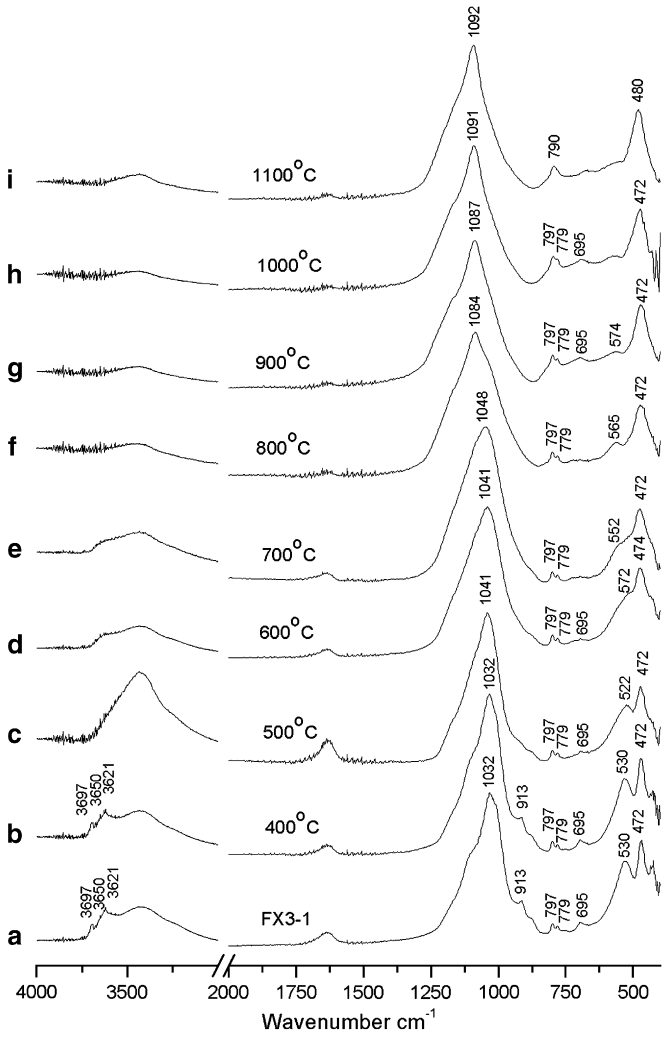

Fig. 5. Infrared spectra of the clay size fraction separated from mud-brick material (sample FX3-1) and heated in a muffle oven for 4 h. (a) Unburned material. (b) Material burned at 400 °C. Despite the reddening of the samples no major Infrared Spectral changes are detected. (c) Material burned at 500 °C: the kaolinite absorptions (3695, 3650, 3620 cm^{-1}) as well as the Al–O–H absorption at 915 cm^{-1} are absent. The Si–O–Si absorption shifts from 1032 to 1041 cm^{-1}, the Si–O–Al band at 520 cm^{-1} is weak and the valley at 495 cm^{-1} is poorly defined. (d) Material burned at 700 °C: the OH montmorillonite absorption at 3620–3630 cm^{-1} is significantly reduced, the main Si–O–Si stretching absorption is shifted further to 1048 cm^{-1} and the Si–O–Al absorption at 520 cm^{-1} is absent. (e) Material burned 800 °C: the spectra show absorptions characteristics of quartz (Si–O–Si bands at 1084 cm^{-1}, Si–O absorption at 800–780 cm^{-1} (doublet), and Si–O band at 470 cm^{-1}) and characteristics of the Al bonds in AlO_4 tetrahedra (at 564 cm^{-1}) derived from the dehydroxylation of the Al $[O(OH)]_6$ octahedra [18]. (f) Material burned at 900 °C: the quartz absorptions weaken and the main Si–O–Si band shifts to 1087 cm^{-1}. (g) Material burned at 1000 °C: the main Si–O–Si band shifts to 1092 cm^{-1}. (h) Material burned at 1100 °C: absorptions characteristic of both opal (at 1092 cm^{-1}) and cristobalite (at 790, 620 and 479 cm^{-1}).

obtained the infrared spectra (Fig. 5). The detailed spectral changes are listed in the legend of Fig. 5.

These results show that the clay-sized fraction alone when heated to temperatures of 800 °C and above, produces spectra that resemble quartz. The tailing of the major peak (1084 cm^{-1}) and the weak absorption of the 510 cm^{-1} absorption are discernible, as was noted for heated total sediments (Fig. 4c). We repeated these heating experiments with a pure montmorillonite standard. From 800 °C and above, the infrared spectra also show quartz absorptions (1084, 695 cm^{-1}), even though quartz itself was absent in the starting material.

Heating of montmorillonite alone does therefore produce spectra that are similar, but not identical to that of quartz. The same heating experiments using standard kaolinite and illite showed the same overall phenomena, but with interesting differences. Fig. 6 is a plot of the shift in the absorption positions of the major Si–O–Si stretching peak as a function of heating temperature of the three standard clays, as well as the clay fraction of the mud-brick material. This shift is an indication of a change in lattice parameters of the clay crystalline structure. The three clay standards behave differently. The mud-brick fraction curve is similar to that of montmorillonite, the major clay type in this sample. This experiment shows that the temperature sensitivity using infrared spectra will be different for sediments containing different clay types. Thus each archaeological site should be ''calibrated'' in this regard using local sediments.

3.2.4. Experimental open fires in the field

As heating sediments in an oven for a limited period of time does not simulate conditions in the field, we also heated FX3-1 mud-brick sediment in a charcoal fire under three different conditions: (a) simple ''domestic'' fire with no bellows; (b) fire augmented with one bellow; (c) fire augmented with two bellows. The times for the total combustion of 2 kg charcoal charge and the maximum and average temperatures reached during the three experiments are shown in Table 2.

Under natural wind conditions the maximum temperature measured was in the known range of open ''domestic'' fire temperatures (below 900 °C). The sediment that was under oxidative conditions turned red, while the sediment that was under reducing conditions turned dark grey/brown to black. The depth to which the heat transfer caused the sediment to change color reached at most 2 cm below the surface. The infrared spectra of the corresponding sediments are shown in Fig. 7a–d. These spectra are comparable with those obtained in the oven experiments up to a temperature of 800 °C (Fig. 4c).

The use of one bellow resulted in temperatures ranging from 1100 to 1300 °C and caused sediment fusion. At the

Table 2
Details and observations of the heating conditions of the experimental fires

Fire type	Duration (h:min)	Temperature (°C)		Sediment color and physical properties
		Average	Max.	
''Domestic'' fire	03:25	570	860	Dark brown–red
One bellow	01:40	1075	1270	Dark brown–red–soil melt
Two bellows	01:05	1310	1450	Dark brown–red–soil melt–glaze

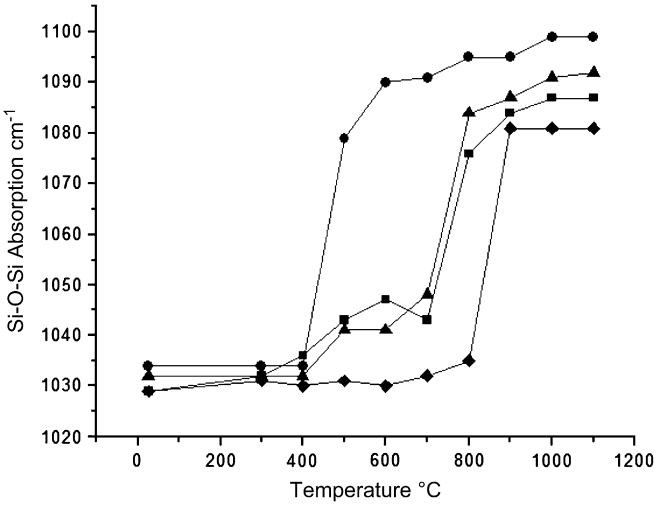

Fig. 6. Shift in the absorption positions of the major Si–O–Si stretching peak as a function of heating temperature of the three standard clays kaolinite (Yang Shan, Suzhon, China) [●], montmorillonite (Otay, California) [▲] and illite (48W1535, Fithian, Illinois) [◆], as well as the mud-brick FX3-1 clay size fraction [■]. This plot shows that if kaolinite is the major clay type in the sediment, then a clear-cut shift in the major absorption is discernible between 400 and 500 °C. For montmorillonite a minor shift occurs between 400 and 500 °C and this is followed by a major shift at temperatures above 700 °C. The peak position of illite only shifts at temperatures above 800 °C. Fig. 6 also shows that the clay size fraction separated from the mud-brick material at Tel Dor (FX3-1) closely follows the trend of montmorillonite.

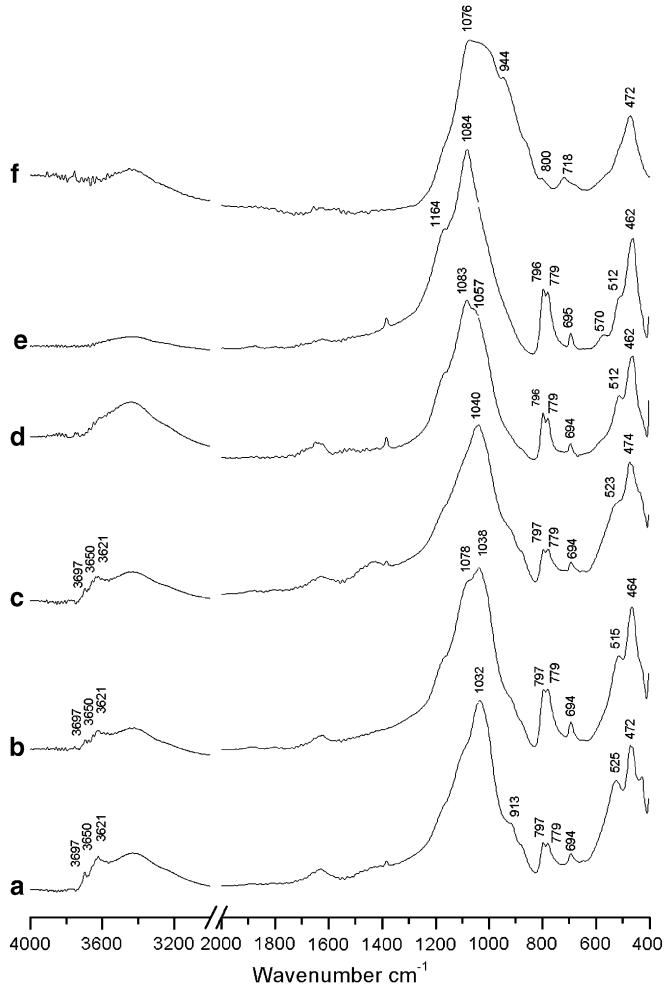

Fig. 7. Infrared spectra of sediments of different colors produced in experimental fires. (a) The unburned sediment used in this experiment. (b) Dark brown sediment. (c) Dark grey sediment. (d) Red sediment. (e) Melted sediment. (f) Glassy phase attached to the crucible.

mouth of the bellow a slag of melted soil formed. The thickness of the reddened sediment underneath the bellow mouth reached a maximum depth of 2.5–3.0 cm. The melted soil infrared spectrum (Fig. 7e) is characterized by quartz-like absorption bands with an additional feature centered at 572 cm^{-1} which is attributed to Al–O bonds from AlO_4 groups of mullite [18]. It also has a less well-defined absorption at 515 cm^{-1}. When two bellows were used a layer, about 3 cm thick, of reddened soil is formed close to the *tuyère* aperture. Some glassy phase is formed on the crucible outer surface at the contact with the ashes. The infrared spectrum of this glassy phase (Fig. 7f) shows a strong Si–O–Si absorption at 1075–1079, 945–950 (shoulder), 718 and 470 cm^{-1}. It is interesting to note that major Si–O–Si absorptions at 1060–1070 cm^{-1} are characteristic of volcanic glasses such as obsidian [34]. Finally, some of the charcoal that was located under the crucible did not combust completely during the experiment. Infrared analysis of the adjacent sediment showed that the associated silicates were not significantly altered.

This study clearly shows that under field conditions, the differences in infrared spectra observed in the oven experiments are indicative of temperatures to which the sediment was exposed. Furthermore, sediments that produce spectra similar to those shown in Fig. 7e and f are likely to be the product of an industry that used bellows for achieving high temperatures. Thus the use of infrared spectroscopy for assessing the approximate temperatures to which clay-containing sediments were heated depends upon the clay type. For Tel Dor sediments exposed to high temperatures, we are able to differentiate five different temperature ranges using infrared spectra. These are summarized in Table 3.

One difficulty in this approach is to differentiate between sediments that were uniformly exposed to high temperatures, and those that are mixtures of unaltered sediments and heated sediments. The infrared spectra of mixed samples will contain strong absorptions from 1033 to 1080 cm^{-1} or higher and a weak absorption around 510 cm^{-1} and the characteristic absorptions around 3600 cm^{-1}. Another difficulty arises from the fact that the common phosphate mineral, carbonated hydroxyl apatite, can mask the main clay absorption peak and cause difficulties in interpreting the effects of heating. Treatment of various samples in this study with solution of hydrochloridric acid (1N HCl) to remove the phosphate mineral did not result in any changes in the clay infrared spectra.

Table 3
Summary of the changes in infrared spectra as a function of heating temperature

Up to 400 °C	Reddened sediment with unaltered clay components
500–700 °C	Loss of kaolinite, dehydroxylation and partial vitrification of smectite
800–900 °C	Quartz with residual altered clay minerals
1000–1200 °C	"Altered quartz", opal, tridymite
1300 °C and above	Glaze like phase, cristobalite

3.3. Application to the eastern section of Area G

The overall studied section is shown in Fig. 2. The part of the section that was examined in detail (Fig. 8) is located in square AI32 and is 3 m wide and 5 m high. A brief review of the local stratigraphy will help to set the samples analyzed in their architectural and chronological contexts. The material is presented from the lowest levels up (for reviews of the Iron Age stratigraphy, chronology and chronological nomenclature at Dor, see [12,24]).

Phases 12–11 belong largely to the latter part of the Late Bronze Age (14th–13th centuries BCE, possibly also to the 12th). This, to date is the only location at Dor were Late Bronze Age deposits have been excavated, and thus the only place were the nature of the LB/Iron Age transition can be elucidated. Assessing the degree of functional continuity in this area between Phases 12–11 and the subsequent Iron Age ones is of major significance, as there is an ongoing debate concerning the degree to which the early Iron Age along this part of the Mediterranean coast signifies a cultural break related to the arrival of new populations [11,25,30]. However, the deposits of Phases 12–11 are the least known in the area due to their partial and incomplete excavation; indeed, Phase 12 is known only from a few soundings. The difference between the two is that Phase 12 is a thick undifferentiated fill, while Phase 11 exhibits several surfaces or tip-lines. The fills characterizing Phase 11 are extremely mixed but fairly consistent across the area: a mix of hard or soft brown and grey sediments and lenses of ash and sand with bits of charcoal throughout. The debris slopes downward from north to south and east to west (i.e. left to right in the section on Fig. 8), suggesting that it was poured/dumped in from a point northeast of the excavated area. Apart from one installation of unclear use to the west of the section (in Phase 11), there is no architecture associated with either of these phases. It is not known whether this is because this area was not built up at this stage or is merely an artifact of the limited exposure. In Phase 11, two copper-based implements were found; a dagger and a ploughshare/adze.

Phase 10 (Ir 1a [*early*]) is much better understood. Based on ceramic chronology it probably mostly encompasses the 11th century BCE and thus there seems to be a chronological gap between it and the preceding Phase 11 (estimated to be 50–100 years based on ceramics), or else an intermediary phase was obliterated/obscured by the Phase 10 construction. A large building was constructed then, which lasted through many changes and one destruction event, to the end of the Iron Age sequence in G, namely Phase 6a of Iron Age II. Wall W18229 in Fig. 8 is one of the walls constructed in Phase 10. To the south (right, on Fig. 8) of this wall is a series of superimposed sloping surfaces marking the central courtyard in the building. The presence of firing pits, a small furnace, a bellows pot, crucible fragments and bits of copper/bronze indicated that in Phase 10 this area was a smithy used for the recasting of copper/bronze objects.

Phase 9 (Ir 1a [*late*]). Chronologically, this phase is very close to the previous one (the 11th and possibly early 10th

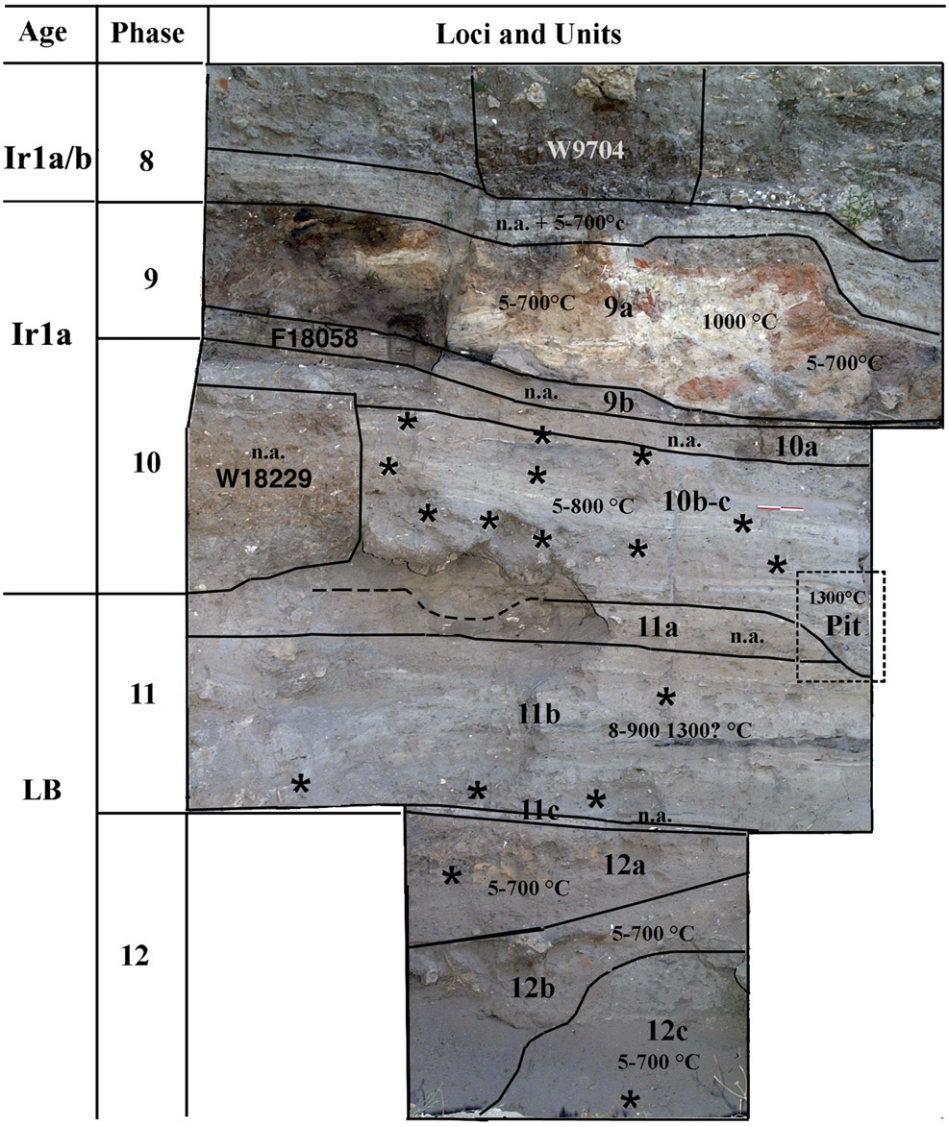

Fig. 8. The part of the eastern section in Area G that was studied in detail. The left-hand column shows the assignment of strata to different stratigraphic phases based primarily on architectural changes. The right-hand side shows a further sub-division of the strata into units, which are discernible based mainly on textural and mineralogical data. In each unit an estimate of the temperature to which the sediments were exposed is given, or if they were not exposed the sediments are designated as not altered (n.a.). The boundaries are superimposed on a photograph of the section itself. The asterisk (*) indicates detectable amounts of copper (0.01 wt% CuO in whole sediment and 0.003 wt% CuO in charcoal fragments).

century BCE). A courtyard building of ''Canaanite'' type was constructed now, utilizing some of the Phase 10 walls. It is dominated by a large courtyard (of which the western half – adjacent to the illustrated section – was partially roofed and partially stone paved), surrounded by rooms on at least three sides. The courtyard may have been used for some stage(s) in the bread-making process, as indicated by the presence of several grinding stones and an unusual trough-shaped installation. This phase perished in a violent conflagration and destruction, which left numerous *in situ* artifacts sealed under the debris. The burnt mud-brick, collapse in the center of the section in Fig. 8, is part of this destruction layer.

Phase 8 (Ir 1a|b) chronologically closely followed the previous phase. It represents a leveling out of the Phase 9 destruction and a rebuilding of walls along the same lines; even the stone pavement is re-established, though on a smaller scale.

Table 4 summarizes the properties of the sediments of the main units exposed in this section. Most of the sediments were exposed to high temperatures. Fig. 8 also shows the estimated temperatures to which these sediments were exposed, using the infrared calibration derived above. As remains of copper producing activities were found associated with some of these layers, we determined the copper contents of all the sediment samples analyzed, and those with detectable amounts of copper (0.01 wt% CuO in whole sediment and 0.003 wt% CuO in charcoal fragments) are also plotted in Fig. 8.

3.3.1. Phases 12–11 (Late Bronze Age)

The Late Bronze Age sediments are exposed in a 3 m deep 2×2 m sounding at the base of the eastern section in Area G (Figs. 2 and 8). Phase 12c, the earliest exposed phase, comprises a 2 m thick compacted sandy brown fill with gravel.

Table 4
Geochemical properties of the archaeological layers and the associated stratigraphic units exposed in the eastern section of Area G at Tel Dor

Age	Phase	Stratigraphic unit	Major mineral components*	Exposure temperatures (°C)	Copper content (CuO Wt %)	Main characteristics
Ir1a late	9	9a (destruction debris)	*Cl(a),* Qz	500–1000	<0.01	Major fire event, *in situ* artifacts. Altered clay, microscopic grains of burned, partially burned and unburned materials, including: *kurkar*, bones, charcoal, mud-bricks, dung, flint, phytoliths, plaster and ash. Authigenic phosphate is also present. Vertical features indicate collapse
		9b (=floor)	*Cl*, *C*, *Q*	Not altered	<0.01	Grey laminae richer in calcite (wood ash?) than brown laminae, one thin laminae is phytolith-rich. Microscopic charcoal, bones (some burned), pottery, kurkar, plaster, flint, shells, authigenic phosphate
Ir1a early	10	10a	*Cl*, C	Not altered	<0.01	
		10b-c pit	*Cl*, *Cl(a),* C, Ch, D	700–900; 1300	0.02–0.18	Casting pit Ash, charcoal, grass phytoliths (burned?), altered clay, copper impregnated bone
		10b-c	*Qz*, *C*, *Ch,* Cl, D	500–800	0.02	Clay curls, Microscopic grains of basalt, kurkar, flint, charcoal, ash, pottery, bones, plaster (?) and mud-bricks
Occupational gap or obliterated phase						
LB	11	11a	*Cl*, Qz, C	Not altered	n.d.	
		11b	*Cl(a),* Qz, C	800–900; 1300	0.04–0.05	Clay curls, altered clay, microscopic grains of basalt, kurkar, flint, charcoal, ash, pottery, bones and mud-bricks
		11c (surface?)	*O*, C	Not altered	<0.01	Micolaminated phytoliths, dung spherulites, authigenic phosphate nodules (i.e., animal dung)
	12	12a	*C*, *Cl(a)*, Ch, Qz	500–700	<0.01	Clay curls, altered clay, microscopic grains of basalt, kurkar, flint, charcoal, ash, pottery, bones and mud-bricks
		12b	*Cl(a),* Qz, C	5–700	<0.01	
		12c	*Cl(a),* Qz, C, Ch	5–700	<0.01	Finely laminated

* The major mineral components are in italics. Cl, clay; Cl(a), clay altered by exposure to heat; Qz, quartz; C, calcite; Ch, charcoal; D, dahllite; O, Opal.

The fill is composed of very finely laminated grey sediments, inter-layered with darker (charcoal-rich) and lighter grey layers. All the sediments have infrared spectra with features indicating exposure to temperatures of 500–700 °C. These layers are cut by a large pit filled with dark reddish brown clayey material and reddened brick fragments and charcoal. The top of the pit is sealed by a 30 cm thick slightly tilted compacted sandy grey/brown fill (Phase 12b).

Phase 12a comprises a dark brown fill mixed with charcoal, orange sediment containing altered clay and black sediment composed of calcite and charcoal. Significant amounts of copper (0.8 wt %) were found associated with the orange colored sediment. This appears to be re-deposited ash (calcite and charcoal) together with burned sediment. Micromorphological analysis shows that the upper 10 cm of Phase 12a includes, from bottom to top: 5 cm thick sub-layer of beach sand that incorporates silt, clay, micritic calcite and charcoal fragments, ca. 2 cm thick sub-layer of pure beach sand, 3 mm thick sub-layer of un-oriented grass phytoliths associated with wood ash and charcoal, and 2.5 cm thick sub-layer of beach sand mixed with silt, clay, micritic calcite, pottery and burned mud-brick fragments. The silt and clay seem to originate from soil (either wind-blown or washed in) and the micritic calcite derives mostly from wood ash. Phase 12a also includes 'clay curls' that are upside down. Clay curls are fragments of sediment that show distinctive graded bedding (from bottom to top: fine sand, silt and clay) that form in low energy aqueous environments (e.g., puddles of rain water). When they are dry and cracked they can be transported by sheet wash, and re-deposited upside down.

An 8 cm thick white layer (11c) crosses the Late Bronze strata. Micromorphology shows that this layer is composed mainly of micro-laminae of grass phytholiths, and contains abundant dung spherulites (sensu Canti [5]) and authigenic phosphate nodules. The infrared spectra confirm the presence of opal (i.e., phytoliths). The micro-laminated structure of phytoliths and its association with dung spherulites indicates that this layer was derived from the degradation of trampled animal dung and may represent a temporary livestock enclosure [22].

Phase 11a-b is a heterogeneous 1 m thick-layered deposit. It contains quartz-rich sandy lenses at the base and a charcoal-rich black lens (11b). The lower part of this unit is composed mainly of heat-altered (800–900 °C) clay, whereas the upper part contains unaltered clay-rich sediments that resemble mud-bricks. The copper contents in the lower part are detectable, whereas in the upper part of this unit copper is below

the detection limit. Micromorphological examination of the lower 9 cm of 11b shows that it is composed of beach sand mixed with silt, clay, wood ash and charcoal, fragments of pottery and burned mud-bricks, and clay curls. This is similar to the top-most part of Phase 12a. The top of this layer (11a) is also problematic in archaeological/chronological terms, as it contained mixed LB and Iron Age potsherds. It is therefore unclear whether it constitutes an LB/Iron Age transitional horizon, or more plausibly based on ceramics, a mixture of LB deposits with later disturbances of the early Iron Age, caused when the Phase 10 building was constructed.

Sediment formation processes: The bulk (bottom) of the sediment deposited (Phases 12c and 11b) was heated to 500–700 °C. It has a fine-grained distinctive powdery texture and is laminated. As no architecture was found in this area in this phase, it appears to have been an open area. There is also no direct evidence of ovens or kilns that could have been the source of the heated sediments. Furthermore, open fires do generally heat sediments to this extent, but certainly not in a uniform manner. The uniform properties may indicate a mixture of sediments. There is thus no clear-cut explanation for these paradoxical observations. We can speculate that this material was the product of some pyrotechnological activities involving ovens or kilns taking place somewhere else, and the sediments were then re-deposited at this location. The repetitive action of re-deposition is responsible for the laminations. The Phase 12a sediments do show additional direct evidence for re-deposition (upside-down curls). In addition, the presence of intact clay curls indicates that the areas where they were formed as well as deposited were not extensively trampled, as trampling would have destroyed them. During the transition between Phases 12 and 11, the area was used as an animal enclosure. There is also ash and charcoal deposition all along the profile. The activities responsible for the production of these heat-affected sediments ceased at the end of this period, and sediments that were not exposed to high temperatures were deposited.

3.3.2. Phase 10 (Ir 1a [Early])

The lower part of Phase 10 is delimited on the north side of the section (Fig. 8) by the remains of an E-W rammed earth, or mud-formed wall (W18229), built of mud-brick material alternating with fieldstone piers, but in which no brick structure was discerned. The clay components are unaltered by exposure to heat. This wall separates a room on the north from the courtyard on the south. This courtyard is included in the section under investigation. As mentioned, the excavation of the courtyard area uncovered a furnace, numerous small size charcoal-rich pits (Figs. 8 and 9) and produced large quantities of bronze objects, copper prills and copper-rich slag remains.

The sediments in the section that are related to the courtyard (10b-c) are grey colored and finely layered. They comprise both heat-altered (500–800 °C) and unaltered clay-rich sediments. Within this sequence are black, grey and brown sandy and ashy sub-layers. Phase 10b-c is characterized by detectable amounts of copper both in the mineral portion of the sediment and in the charcoal fragments. The white thin sub-

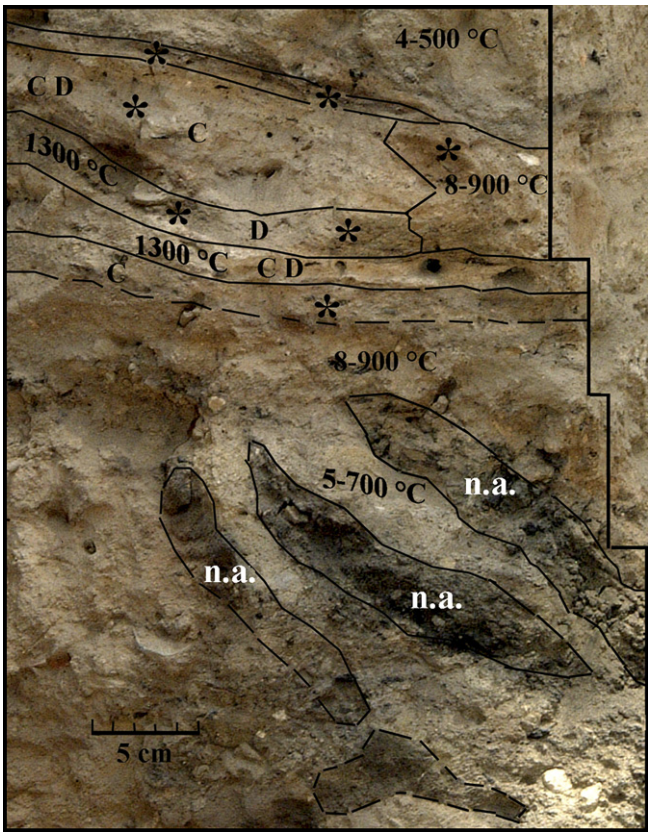

Fig. 9. Details of one of the pits exposed in the eastern section of Area G in Phase 10b-c. Photograph of the pit with superimposed interpretation of the different units (C, Calcite; D, carbonated apatite (dahllite)) and the estimated temperatures to which each was exposed (n.a. = not altered). The asterisk (*) indicates detectable amounts of copper (0.01 wt% CuO in whole sediment and 0.003 wt% CuO in charcoal fragments).

layers contain calcite and high temperature silicate phases with major Si–O–Si absorptions at 1040–1050 cm^{-1} and 1072–1075 cm^{-1}, indicating that they were formed at a temperature as high as 1300 °C.

The details of the pit on the south side of the section in Phase 10b-c are shown in Fig. 9. The bottom of this pit is defined by a layer of charcoal. The top of the pit is characterized by a light grey layer inter-bedded by centimeter thin dark layers. Reddened sediment is also present. Micromorphological analysis shows that the top part of the pit is composed mainly of calcitic wood ash, mixed with burned grasses and quartz sand. Some calcite from the ash dissolved and moved a few centimeters down the profile, filling in the voids. The sediments above and below the pit have higher contents of sand (20–30%) and contain clay curls. Infrared spectra show that the sediments associated with charcoal at the base of the pit are not altered. Some of the reddened sediment shows alteration due to temperatures of 700–900 °C. The white material at the top of the section is composed of calcite (probably wood ash) with trace amounts of carbonated apatite. The centimeter thick dark layers that lie between the calcitic layers contain glassy material similar to that produced experimentally by augmenting the fire at 1300 °C with two bellows (Fig. 7f). No copper was detected in the charcoal and the

adjacent reddened sediment at the bottom of the pit. On the other hand, the white calcitic wood ash, the reddened sediment and the dark glassy phases at the top of the pit have significant amounts of copper that range between 0.02 and 0.18 wt % Cu. We note that within this pit a green-colored bone fragment impregnated with copper was found.

The upper layer (10a) of Phase 10 stratum is composed of clay-rich sandy material that does not contain any high temperature silicate phases or copper.

Sediment formation processes: This open courtyard contains mainly burned sediments, together with many shallow charcoal-rich pits. A detailed analysis of one of these pits shows the presence of high concentrations of copper, and sediments that were heated to very high temperatures. These observations are consistent with the pits having been used for casting copper-rich metal objects. The large amounts of wood ash indicate the use of large quantities of fuel for the operation of the casting pit. This interpretation is also consistent with many copper-containing prills and slags that were found in Phase 10b-c. The presence of clay curls in Phase 10, as in Phases 12 and 11, indicates that the area was not trampled extensively, i.e., relatively low human/animal traffic. It is clear that the casting pits identified in Phase 10 are *in situ*, but it is still unclear whether the other sediments composing this phase are *in situ* or re-deposited.

3.3.3. Phase 9 (Ir 1a [Late])

Phase 9 is characterized by heavily burned architectural features that were exposed to a large fire that was also evident in other excavation areas. This fire destroyed significant parts of the *tell*. Phase 9 is identifiable by a centimeters thick charcoal-rich black layer that crosses the entire section and is designated as the ''the destruction layer''.

The base of Phase 9 (9b) is composed of thin sub-layers (referred to as a ''tan multiple floor''), whose top (F18058) is darkened by the effect of the fire. Micromorphological analysis shows that the laminations are alternations of layers rich or poor in clay and calcite relative to the quartzitic beach sand substrate, where dark-colored brownish layers are richer in clay and light-colored greyish layers are richer in calcite. The calcite seems to be derived, at least partially, from wood ash and probably also burned grass (i.e., slender elongated charcoal fragments associated with grass phytoliths). The infrared spectra show that all the laminations contain unaltered clay minerals, indicating that these surfaces were either prepared or formed naturally with fresh clay, ashes and beach sand. The manner in which these multiple layers formed is not known. The sediment on the surface of Phase 9b and in close contact with the charcoal and heat-affected sediments were exposed to temperatures above 500 °C. The ceramics found *in situ* on the floor were lying directly on a white-colored 1–2 mm thick layer composed of opaline grass phytoliths. Micromorphological analysis of the Phase 9a (destruction) sediments shows a mixture of burned, partially burned and unburned materials, including vegetal matter, kurkar, mud-bricks, flint, plaster, phytoliths, spherulites and ash. Burnt mud-brick fragments have vesicular fabric due to the degassing at temperature above 750 °C of calcite and aragonite composing the kurkar inclusions. Certain features appear in a sub-vertical position, indicating collapsed materials. One such feature is, notably, composed of animal dung (very large amounts of spherulites) and may represent dung plaster or a collapsed dung plastered roof. Authigenic phosphate nodules are present in association with the dung remains, and some may have been burned as well. Sub-vertical, thin, phytolith-rich layers are also present, and are found above the spherulite-rich sub-vertical layer. A feature identified in the field by the excavators as a possible collapsed roof is composed of mud-brick material mixed with calcite (probably wood ash). Horizontal laminae of phytoliths and spherulites were also identified, and in addition, areas rich in groups of phytoliths, each in a different orientation. The combination of all the remain types, their apparent burned state, and the presence of a mixture of sub-vertical and sub-horizontal orientations testify that quite a large amount of materials (apart from the mud-brick walls) had collapsed during the Phase 9 destruction.

The remains of a large collapse of architecture (1.8 × 0.8 m) that consists of reddened mud-bricks and yellowish white sediment (9a) are located on the surface of Phase 9b. The infrared spectrum (Fig. 3d) of the yellowish white sediment at the center of the collapsed feature is composed of silicate minerals containing glassy phases that must have formed above 1000 °C. The red-colored sediments contain phases produced at temperatures ranging from 500 to 1000 °C. Both the white- and red-colored sediments appear to have been derived from mud-bricks, and the color differentiation also reflects a temperature gradient. No significant amounts of copper are present.

Sediment formation processes: Phase 9 (units 9a and b) sediments are the products of partially collapsed mud-brick architectural features and many other materials, notably wooden beams and possibly a roof, that have been exposed to a very substantial temperature gradient due to a fire. Due to the catastrophic circumstances of their formation, these sediments are clearly *in situ* and not re-deposited.

3.3.4. Phase 8 (Ir 1a/b and 1b)

Phase 8 represents the rebuilding of the house after the destruction. It consists of wavy laminated sediments that overlie a 5 cm thick sub-layer composed of clay-rich material. Infrared analysis shows that the clayey material is unaffected by heat.

3.3.5. Waste products from the copper-based industry in Area G

In the course of excavation of Phases 12–9 in Area G, around 200 ''waste products'' were collected manually. These included mostly small metal chunks and prills, identified by their greenish appearance, as well as several crucible fragments. The entire collection was sorted visually and using an X-ray fluorescence (XRF) analyzer. The latter enabled us to verify the copper content of the products and to remove tainted stones, sherds, bone fragments and shells. Table 5 presents the distribution of the waste products in the various phases. It distinguishes between 0.3–3 cm spherical pieces

Table 5
The number of waste products from the copper-based industry in Phases 9–12 in Area G at Tel Dor

Phase	Prills	Lumps	Worked	Crucible	Total	Other
8	–	–	–	–	0	
9	4	2	3	–	9	–
10	82	48	6	5	141	1
11	2	10 (including 1 possible ore fragment)	7	1	20	2
12	8	8	2	1	19	–
Total	96	68	18	7	189	3

(designated ''prills'') and various sized amorphous lumps. It should be stressed that due to the humid climate of Tel Dor, corrosion has severely affected most of the artifacts. 'Lumps' may therefore be distorted prills or even fragments of worked bronze that were totally corroded. It should also be noted that the only complete crucible found was in L18313, Phase 10. Most of the material comes from Phase 10 (Table 5). This correlates well with the architectural finds of Phase 10, which included various installations that may have been used for the re-melting of bronze, as well as the copper content distributions in the sediments of the eastern section (Fig. 8). The small number of waste products found in Phases 11 and 12 may certainly, in part, reflect the fact that less volume was excavated from these phases compared to Phase 10. This however is not the case for Phase 9.

4. Discussion

Our analyses of sediments from different locations and from different periods at Tel Dor, clearly showed the widespread presence of sediments that have been affected in one way or another by exposure to high temperatures. We recognized this from infrared spectra based on previous studies mainly by Farmer [9] and Shoval [26,27]. This study therefore provides a better understanding of the relations between the minerals deposited on the *tell* and exposure to heat, and then applies this information to the study of sediments in a particular section.

Our laboratory studies established the effect of heat on mud-brick materials, and more specifically on the clay fraction of the mud-brick materials. This resulted in a series of infrared spectra that were produced by heating mud-brick sediments in an oven for 4 h. Using infrared spectra, we can clearly distinguish heating temperatures within a range of about 200 °C. We also show that this calibration is directly affected by the clay types, and should be repeated when applied to other archaeological sites. The relevance of this ''calibration'' to actual heating in natural fires was established by a series of open-air experiments using fires with and without bellows.

In this study most of the soils that were affected by heat are not red colored, except for the localized patch in the Area G section (Phase 9) that actually surrounds white-yellow colored sediments that were heated to even higher temperatures. Moreover, most heat-affected sediments identified in this study are grey colored, which based on the micromorphological observations may be attributed to the fact that they are extensively mixed with wood ash and microscopic charcoal. This is consistent with the observations and discussion of Canti and Linford [6].

We note that phosphate-rich solutions can cause alteration of clay minerals, and intense phosphatization will result in the dissolution of clays with the formation of authigenic amorphous silica (e.g. opal) [17]. Clay minerals can also be altered and dissolved by acid solutions [16]. The clay minerals in some of the Middle Paleolithic sediments (Layer F) in Hayonim cave (Israel) have infrared spectra similar to the one produced by heating the mud-brick clay fraction to 500–700 °C. The presence in Hayonim Cave of large quantities of opal and several phosphate phases associated with the altered clays [35], shows that in this case the clay alteration is due to chemical diagenesis and not of heat. Thus when studying the effect of heat on clay-rich sediments it is necessary to rule out other possible causes of clay mineral diagenesis.

We demonstrated the use of this approach for better understanding the effect of heat on sediments by studying one section in Area G of Tel Dor in detail. This example shows three fundamentally different ways that heat-affected sediments can be produced. In the Late Bronze Age (Phases 11–12), the sediments were heated somewhere else and were then deposited in the area under investigation. These sediments were all heated to temperatures of between 800 and 900 °C. Whereas our field experiments demonstrate that this can be achieved in an open fire without the use of bellows, it is not obvious how such large volumes of heat-affected sediments could have been produced in an open fire. Only the top centimeter or two of the sediments beneath such a fire are affected by heat to this extent. It is conceivable that if domestic cooking fires were repeatedly produced on a layer of sediment that between firing events was mixed up, this would eventually produce large volumes of such heat-affected sediments. A more plausible scenario is that these sediments were exposed to heat from ovens or kilns. We also noted that detectable amounts of copper were only associated with the base of the section. This suggests that most, but not all of the heat-affected sediments was unlikely to be related to the manufacture of copper-containing materials.

The second mode of formation of heat-affected sediments observed in the section was clearly due to the production of copper-containing materials in the area of the section (Phase 10). The association of what appears to be casting pits together with copper slags and prills shows that in the first phase of the Iron Age this area was used for metal production (see Shalev [23] for an archaeometallurgical study of similar archaeological remains from the same period at Tel Dan, as well as a proposed reconstruction mode). The casting presumably affected the local sediments. From the infrared analysis, it is clear that bellows must have been used to produce such high temperatures in the pits. A bellows pot was indeed found in Phase 10.

There is abundant evidence that in Phase 9 of the early Iron Age, a major conflagration occurred in this area. The infrared spectra of sediments from the section certainly confirm this

and identify the location of the core of the fire preserved along this north–south section. The temperatures reached (around 1000 °C) are very high. Archaeological observations from this area support the notion that these heat-affected sediments were produced *in situ* at this location.

It is interesting to note that boundaries between archaeological Phases 11 and 10 and Phases 10 and 9, that were designated during the excavation of this area based mainly on architectural considerations, are both immediately above relatively thin layers of sediments that were unaltered by exposure to heat. This implies that the pyrotechnological activities that were responsible for affecting the bulk of the sediments in each phase, ceased for some period of time, before the next activity/event occurred. It is conceivable that the sediment deposition rate during these periods of unaltered sediment deposition was slow due to the absence of human activities on the *tell*, such as importing and/or dispersing sediments, producing ash from fires and maintaining animals. These relatively thin layers could therefore represent disproportionately longer periods of time. On the other hand, it is possible that they represent short periods of time, if these layers are composed of raw mud-brick material brought in during a fast constructional phase. This latter scenario is more consistent with the ceramic record.

It is also significant that there is a substantial change in sediment composition at the boundaries between the architecturally defined stratigraphic phases. This implies that redeposition of sediments, and the artifacts within them, was less significant than expected in such a continuously occupied building (and where living horizons consisted mainly of dirt floors). This is crucial for assessing the degree of residuality of artifacts, and concomitantly their chronological and systemic association to the architectural units they relate to.

5. Concluding comments

Large volumes of sediments at Tel Dor have been exposed to high temperatures. By heating local sediments in an oven and performing open fire experiments, we could ''calibrate'' the changes observed using infrared spectroscopy as a function of temperature. Using this information, we show that the circumstances in which sediments are exposed to high temperatures can vary. In some cases there is ample archaeological evidence associated with the sediments to infer how the high temperature exposure occurred. There are however many sediment accumulations where the only evidence for pyrotechnology is from the sediments themselves. Detailed analysis of these sediments may be an invaluable means of reconstructing fire-associated activities even when the actual installations have not been exposed during the excavation or were not preserved.

Acknowledgements

Between 1980 and 2000 Tel Dor was excavated by E. Stern of the Hebrew University, Jerusalem, heading an international consortium of universities supported by the Berman Foundation for Biblical Archaeology. The Late Bronze Age deposits were largely excavated under the supervision of Elisabeth Bloch-Smith of Gratz College, Philadelphia and Willem Boshoff, the Department of Old Testament, University of South Africa, and the Iron Age phases by groups from the University of California at Berkeley and Cornell University, headed by Andrew Stewart and Jeff Zorn. John Berg of the Farwestern Anthropological Research Group and Talia Goldman and Svetlana Matskevitch, both from the Hebrew University, took part in supervising, recording and analyzing the stratigraphy of the sampled contexts. We thank Natalia Lyashenko and all the members of the Kimmel Center for Archaeological Science at the Weizmann Institute for their help in sampling and analyzing bulk sediment samples using the on-site infrared spectrometer. This study was funded in part by generous support from Mr. George Schwartzmann, Sarasota, Florida, and by the Kimmel Center for Archaeological Science at the Weizmann Institute. F. Berna is the beneficiary of a European Union Marie Curie Fellowship. S.W. is the incumbent of the Dr. Trude Burchardt professorial chair of Structural Biology.

References

[1] J.M. Alia, H.G.M. Edwards, F.J. Garcia-Navarro, J. Parras-Armenteros, C.J. Sanchez-Jimenez, Application of FT-Raman spectroscopy to quality control in brick clays firing process, Talanta 50 (1999) 291–298.
[2] R.V. Bellemo, J.W.K. Harris, Preliminary report of actualistic studies of fire within Virunga National Park, Zaire: towards an understanding of archaeological occurrences, in: N.T. Boaz (Ed.), Evolution of Environments and Hominidae in the African Western Rift Valley 1, Virginia Museum of Natural History Memoir, Martinsville, 1990, pp. 317–338.
[3] H.J. Bray, S.A.T. Redfern, Kinetics of dehydration of Ca-montmorillonite, Physical Chemistry of Minerals 26 (1999) 591–600.
[4] P. Bullock, N. Federoff, A. Jongerius, G. Stoops, T. Tursina, U. Babel, Handbook for Soil Thin Section Description, Waine Research, Wolverhampton, 1985.
[5] M.G. Canti, The production and preservation of faecal spherulites: animals, environment and taphonomy, Journal of Archaeological Science 26 (1999) 251–258.
[6] M.G. Canti, N. Linford, The effects of fire on archaeological soils and sediments: temperature and colour relationships, Proceedings of the Prehistoric Society 66 (2000) 385–395.
[7] W.M. Carty, U. Senapati, Porcelain – raw materials, processing, phase evolution, and mechanical behavior, Journal of the American Ceramics Society 81 (1998) 3–20.
[8] M.A. Courty, P. Goldberg, R. MacPhail, Soils and Micromorphology in Archaeology, Cambridge University Press, Cambridge, 1989.
[9] V.C. Farmer (Ed.), The Infrared Spectra of Minerals, Mineralogical Society Monograph, London, 1974.
[10] G.W. Gee, J.W. Bauder, Particle-size Analysis, in: A. Klute (Ed.), Methods of Soil Analysis Part I: Physical and Mineralogical Methods, Soil Science Society of America, Inc., Madison, 1986.
[11] A. Gilboa, Sea Peoples and Phoenicians along the Southern Phoenician Coast - a reconciliation: an interpretation of Šikila (SKL) material culture, Bulletin of the American Schools of Oriental Research 337 (2005) 47–78.
[12] A. Gilboa, I. Sharon, An archaeological contribution to the Early Iron Age chronological debate: alternative chronologies for Phoenicia and their effects on the Levant, Cyprus and Greece, Bulletin of the American Schools of Oriental Research 332 (2003) 7–80.
[13] D. Kadosh, D. Sivan, H. Kutiel, M. Weinstein-Evron, A late quaternary paleoenvironmental sequence from Dor, Carmel coastal plain, Israel, Palynology 28 (2004) 143–157.
[14] P. Karkanas, M. Koumouzelis, J.K. Kozlowksi, V. Sitlivy, K. Sobczyk, F. Berna, S. Weiner, Aurignacian clay hearth structures in Kleisoura

cave 1, southern Greece: the earliest evidence of clay use, Antiquity 78 (301) (2004) 513–525.
[15] S. Klein, A. Hauptmann, Iron Age leaded tin bronzes from Khirbet Edh-Dharih, Jordan, Journal of Archaeological Science 26 (1999) 1075–1082.
[16] J. Madejova, FTIR techniques in clay mineral studies, Vibrational Spectroscopy 31 (2003) 1–10.
[17] O.J. Nriagu, Phosphate-clay mineral relations in soils and sediments, Canadian Journal of Earth Sciences 13 (1976) 717–736.
[18] H.J. Percival, J.F. Duncan, P.K. Foster, Interpretation of the kaolinite-mullite reaction sequence from infrared absorption spectra, Journal of the North American Ceramic Society 57 (1974) 57–61.
[19] K. Ramaswamy, M. Kamalakkannan, Infrared study of the influence of temperature on clay minerals, Journal of Thermal Analysis 44 (1995) 629–638.
[20] P. Rice, Pottery Analysis. A Source Book, The University of Chicago Press, 1987.
[21] A. Rosen, Cities of Clay – The Geoarchaeology of Tells, The University of Chicago Press, 1986.
[22] R. Shahack-Gross, R.M. Albert, A. Gilboa, O. Nagar-Hilman, I. Sharon, S. Weiner, Geoarchaeology in an urban context: the uses of space in a Phoenician monumental building at tel Dor (Israel), Journal of Archaeological Science 32 (2005) 1417–1431.
[23] S. Shalev, Metal production and society at Tel Dan, in: Biblical Archaeology Today, Proceedings of the Second International Congress on Biblical Archaeology, Supplement, Israel Exploration Society, 1993, pp. 57–65.
[24] I. Sharon, A. Gilboa, The SKL town: Dor in the Early Iron Age, in: M. Artzy, A.E. Killebrew, G. Lehmann (Eds.), Philistines and Other Sea Peoples, Brill, Leiden, in press.
[25] E.S. Sherrat, ''Sea Peoples'' and the economic structure of the Late Second Millennium in the Eastern Mediterranean, in: S. Gitin, A. Mazar, E. Stern (Eds.), Mediterranean Peoples in Transition, Thirteenth to Early Tenth Centuries BCE, In Honor of Professor Trude Dothan, Israel Exploration Society, Jerusalem, 1998, pp. 292–313.
[26] S. Shoval, The burning temperature of a Persian-Period pottery kiln at Tel Michal, Israel, estimated from the composition of slag-like material formed in its wall, Journal of Thermal Analysis 39 (1993) 1157–1168.
[27] S. Shoval, The firing temperature of a Persian-Period pottery kiln at tel Michal, Israel, estimated from the composition of its pottery, Journal of Thermal Analysis 42 (1994) 175–185.
[28] S. Shoval, M. Boudeulle, S. Yariv, L. Lapides, G. Panczer, Micro-Raman and FT-IR spectroscopy study of the thermal transformations of St. Clair dickite, Optical Materials 16 (2001) 319–332.
[29] A. Smith, Bonfire II: The return of pottery firing temperatures, Journal of Archaeological Science 28 (2001) 991–1003.
[30] L.E. Stager, The impact of the Sea Peoples (1185–1050), in: T.E. Levy (Ed.), The Archaeology of Society in the Holy Land, Leicester University Press, London, 1995, pp. 332–348.
[31] E. Stern, Dor-Ruler of the Seas, Israel Exploration Society, 2000.
[32] M. Tite, A. Shortland, S. Pynter, The beginnings of vitreous materials in the Near East and Eygpt, Accounts of Chemical Research 35 (2002) 585–593.
[33] A. Tsatskin, A. Ronen, Micromorphology of a Mousterian paleosol in aeolianites at the site Habonim, Israel, Catena 34 (1999) 365–384.
[34] H.W. Van der Marel, H. Beutelspacher, Atlas of Infrared Spectroscopy of Clay Minerals and Their Admixtures, Elsevier, New York, 1976.
[35] S. Weiner, P. Goldberg, O. Bar-Yosef, Three dimensional distribution of minerals in the sediments of Hayonim Cave, Israel: diagenetic processes and archaeological implications, Journal of Archaeological Science 29 (2002) 1289–1308.
[36] T. Wertime, Man's first encounters with metallurgy, Science 146 (1964) 1257–1267.